

Unusual regiodivergence in metal-catalysed intramolecular cyclisation of γ -allenols†

Jannine L. Arbour, Henry S. Rzepa,* Andrew J. P. White and King Kuok (Mimi) Hii*

Received (in Cambridge, UK) 6th July 2009, Accepted 10th September 2009

First published as an Advance Article on the web 13th October 2009

DOI: 10.1039/b913295c

Different O-heterocycles can be obtained from a common γ -allenol precursor by using Ag, Zn or Sn catalysts; the results were rationalised by molecular modelling.

Intramolecular hydroalkoxylation of γ -allenols **1** can potentially afford 5- or 6-membered O-heterocycles **2** or **3** via different mechanistic pathways (Scheme 1):¹ the former (5-*exo*-trig) cyclisation is more common, and can be obtained using Pt^{2a} or Au^{2b} catalysts, including enantioselective reactions,³ through π -activation of the C=C bond. Conversely, the only known catalytic example⁴ of a 6-*endo*/*exo*-dig cyclisation was achieved at 130 °C using a lanthanide amide complex via C=C insertion into Ln–O.⁵

In this communication, we report an unusual observation in the intramolecular cyclisation of γ -allenols, where the regiochemistry of the process can be altered by using different metal catalysts.^{6,7}

The work initiated with the observation that γ -allenol **1a** underwent 5-*exo*-trig cyclisation in the presence of a catalytic amount of AgOTf to afford **2a**.⁸ Subsequent screening of metal triflates led to the serendipitous discovery of two catalysts that effect complementary 6-*exo*-dig selectivity (Scheme 2). Under virtually identical conditions, Sn(OTf)₂ transformed **1a** into benzopyran **4** via tandem C–O/C–C bond formations, while Zn(OTf)₂ favoured sequential C–O formations to furnish the acetal structure **5** at a higher temperature (structures **4** and **5** were verified by X-ray crystallography, see the ESI†). Although small amounts of **2a** were detected in both reaction mixtures (6 and 13%, respectively), **2a**, **4** and **5** did not interconvert when left exposed to the other catalysts, suggesting the operation of competitive and irreversible processes.

The regiodivergence of these catalytic systems was similarly observed with substrates **1b** and **1c** (Scheme 3, Table 1): while AgOTf provided tetrahydrofurans **2b** and **2c** (entries 1 and 6), corresponding reactions using Sn(II) and Zn(II) triflates afforded tetrahydropyran rings as major products at ambient temperature (entries 2, 4 and 8). In the case of **1b**, a mixture of double bond isomers **6a** and **6b** was obtained, acetal formation was presumably prohibited for steric reasons. Rate of the

Sn-mediated reaction was attenuated by replacing the diphenyls in **1a** with a cyclohexyl group **1c**, such that 5-membered ring formation became competitive (entry 7). The reaction catalysed by Zn(OTf)₂ was also sluggish at room temperature, although the larger ring was still preferred (entry 8). At a higher temperature, selectivity for the 6-membered ring product remained unchanged for the system catalysed by Sn(OTf)₂ (entries 2 vs. 3), while there was a switch in favour of the smaller ring by Zn(OTf)₂ (entries 4 vs. 5 and 8 vs. 9).

Brønsted acid catalysis was investigated by addition of 30 mol% triflic acid to **1a**. At room temperature, the formation of **4** was observed in a lower yield (50%, r.t., 23 h) compared to Sn(OTf)₂.⁹ Likewise, acid-catalysed cyclisation of **1b** led to **6a** and **6b** (1 : 6 ratio). However, substrate **1c** remained inert over 6 days (r.t.). These observations, accompanied by the switch of selectivity for the 5-*exo*-trig compound at higher temperatures for the Sn and Zn systems, suggest that a H⁺-catalysed process is not likely to be significant.

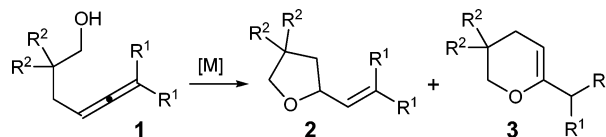
DFT-based models were employed to provide a rationale for the observed regiodivergence. Using γ -allenol **1a** as substrate, with the counter-ion modelled as triflate (L = OTf, X = SO) or trifluoroacetate (L = TFA, X = C), the 5-*exo*-trig transition state (TS1, Scheme 4) resulting in **2a** was tested on group 11 metals (Cu, Ag and Au), for which there is reliable experimental data. At the B3LYP/cc-pVDZ level of theory (cc-pVDZ-pp for the metal), the activation free energies (ΔG^\ddagger) for TS1 (L = TFA) were calculated to be 26.7, 18.1 and 12.2 kcal mol⁻¹, respectively, commensurate with experimental observations that gold-catalysed reaction occurs at sub-ambient conditions, silver at room temperature, and no reaction was observed with copper under ambient conditions.

Calculated transition normal modes, illustrated as animations in the web-enhanced Table 1 (M = Cu, Ag, Au) and statically (Fig. 1), reveal that C–O bond formation is assisted by concomitant deprotonation of the OH group by the adjacent carbonyl of the ligand, the reaction completing with a protonolysis of intermediate **I** (TS5). Modifying L = OTf to L = TFA is predicted to reduce the barrier by 1.5 kcal mol⁻¹, corresponding to a rate increase of ca. 12-fold at ambient temperature. Indeed, this was verified experimentally: **1a** underwent complete cyclisation in the presence of 15% of

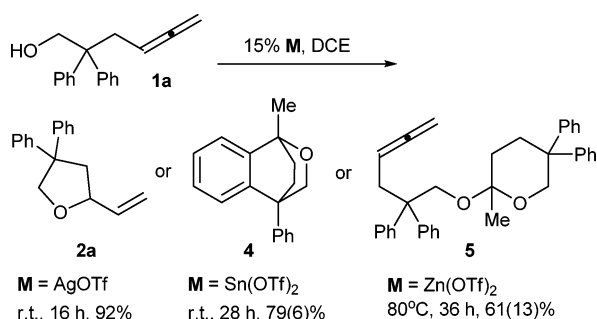
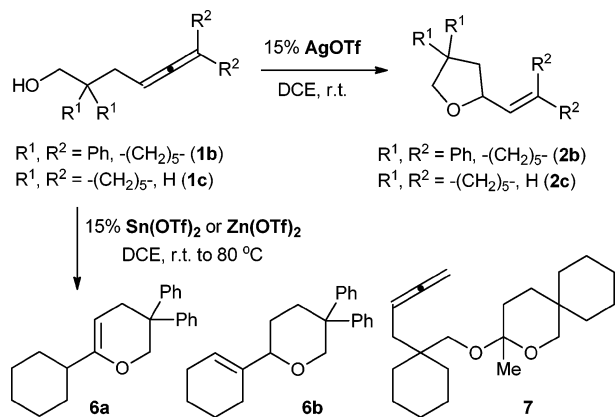
Department of Chemistry, Imperial College London, Exhibition Road, South Kensington, London SW7 2AZ, UK.

E-mail: rzepa@imperial.ac.uk, mimi.hii@imperial.ac.uk

† Electronic supplementary information (ESI) available: Crystallographic data for compounds **4** and **5**, experimental procedures, and compound characterization (pdf). CCDC 726110 & 726111. For ESI and crystallographic data in CIF or other electronic format see DOI: 10.1039/b913295c. Calculated coordinates and animated transition state normal modes are provided via web-enhanced tables via the HTML version of the article.



Scheme 1 5-*exo*-trig and 6-*exo*-dig cyclisation of γ -allenols.

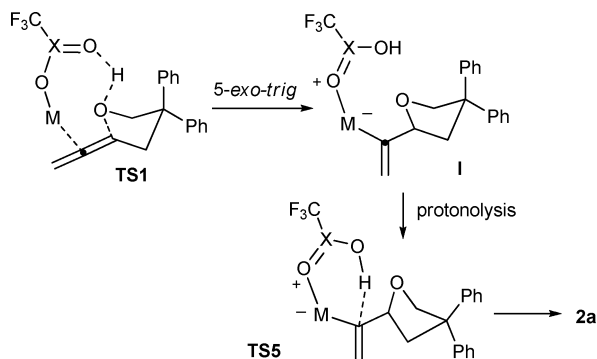
Scheme 2 Metal-catalysed cyclisation of **1a**.

Scheme 3 5- vs. 6-Membered ring formation.

Table 1 Cyclisation of γ -allenols **1b** and **1c** using different catalysts^a

Entry	Precursor	Catalyst	Product	<i>t</i> /h	<i>T</i> /°C	Yield ^b (%)
1	1b	AgOTf	2b	18	r.t.	82
2		Sn(OTf) ₂	6a : 6b (1:9.25)	28	r.t.	82 (6)
3			6a : 6b (1:8.3)	34	50	84 (2)
4		Zn(OTf) ₂	6a : 6b (1:11.5)	28	r.t.	75 (9)
5			6a : 6b (1:1)	34	50	15 (70)
6	1c	AgOTf	2c	12	r.t.	76
7		Sn(OTf) ₂	7	144	35	29 (40)
8		Zn(OTf) ₂	7	144	r.t.	45 (9) ^c
9		Zn(OTf) ₂	7	36	50	9 (52)

^a Typical reaction conditions: γ -allenol (0.4 mmol) in DCE (0.3 mL), catalyst (0.06 mmol, 15 mol%). ^b Isolated yields after column chromatography. Values in parenthesis denote (isolated) yields of the 5-*exo*-trig compound. ^c **1c** recovered in 25% yield.

Scheme 4 Proposed pathway for 5-*exo*-trig cyclisation.

Ag(TFA) at room temperature within 2 h to furnish **2a** in 90% isolated yield (compared to 16 h by AgOTf, Scheme 2).

Possible mechanistic pathways leading to the formation of 6-membered rings are shown in Scheme 5: TS2 was initially proposed as a pathway to product **4**, involving electrophilic activation of the allene, followed by aromatic substitution *via* deprotonation of the Wheland intermediate. Alternatively, the reaction can proceed *via* TS3, where C–O bond formation is followed by protonolysis, resulting in a cyclic enol ether intermediate, which can be trapped by another molecule of **1a** to give **5**. An alternative to protonolysis is internal proton transfer (**II** to **III**, *via* TS6) followed by aromatic substitution involving C=O⁺ as electrophile (TS4), accompanied by synchronous deprotonation of the nascent Wheland intermediate to give **4**. The calculations (web-enhanced Table 1, M = Cu, Ag, Au) reveal that TS1 is lower in free energy than TS2 and TS3 for the group 11 metals, in accord with formation of the kinetic product **2a** rather than **4** or **5**.

Modelling studies for divalent metals are more complex and subtle, with either tetrahedral (Zn) or hemi-directed (Sn) metal coordinated by two bidentate ligands replacing the linear coordination of the group 11 metals, and the possibility of additional coordination to the metal. Annotated geometries for these are set out in web-enhanced Table 2. In all cases, TS2 is higher in free energy than the other pathways (TS1 and TS3), and can be discounted from further discussion. For M = Zn, the metal is essentially tetrahedral, achieving this *via* one Zn–C and three Zn–O bonds (from one bidentate and one monodentate ligands). The remaining oxygen from the monodentate ligand acts as the base for proton removal (Fig. 1). TS3 (M = Zn) is now lower in free energy than TS1 (the reverse of that computed for M = Ag), and is assisted by an additional moderate Zn···OH interaction (~2.5–02.6 Å) not present in TS1. With this metal, the product resulting from TS3 (**5**) is indeed that observed. Conversely, a different geometry is found for TS3 when M = Sn. Rather than being tetrahedral, the hemi-directed metal coordination sphere comprises one Sn–C and two Sn–O bonds resulting from monodentate coordination of TFA or OTf, augmented by two much weaker (~3.0–3.1 Å) Sn–O interactions (web-enhanced Table 2). The product observed with the Sn catalyst is not **2a** or **5**, but **4**. With the high energy TS2 not providing a route to the observed product, we focused on TS4 (Fig. 1) as a possible pathway for C–C bond formation. This represents an electrophilic aromatic substitution *via* a mechanism in which the loss of aromaticity, implied by formation of a discrete Wheland intermediate, is minimised by conflating the C–C bond formation with synchronous deprotonation by an appropriately located oxygen atom from one of the ligands.¹⁰ Such mechanistic synchronicity has also recently been suggested¹¹ for aromatic electrophilic metallations involving C–metal bond formation; our observation extends this mechanistic type to add an example of C–C bond formation. The geometry at the Sn is again notable for a weak (2.90 Å) Sn–O interaction augmenting the normal coordination. Nevertheless, the relative energy of TS4 emerged as higher than that of TS1 or TS3. As apparent from Scheme 5, however, TS4 involves a greater degree of charge separation than the other transition

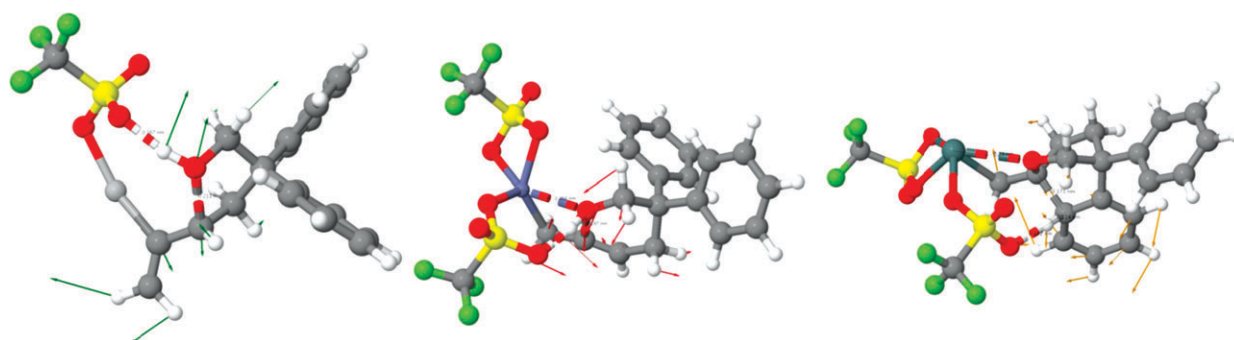
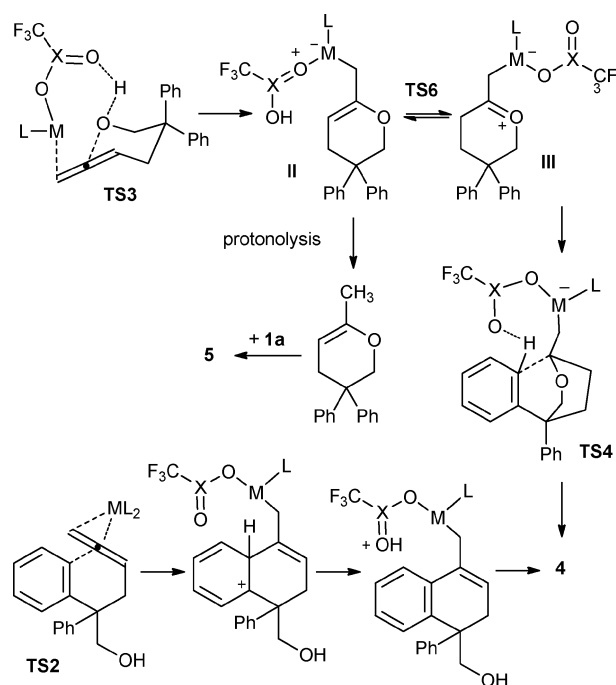


Fig. 1 Calculated normal transition mode for the cyclisation of **1a**: TS1 (left, M = Ag), TS3 (middle, M = Zn) and TS4 (right, M = Sn), L = OTf. Animations of calculated transition modes are presented in web-enhanced Tables 1 and 2 (see the online version).



Scheme 5 Proposed pathways for 6-*exo*-dig cyclisations.

states, and indeed the (gas phase) computed dipole moments are in the region of 12–15 D (compared to 7–10 D for the other transition states). Performing a continuum solvation energy correction for dichloroethane as solvent significantly reduced the relative energy of TS4 (L = OTf) to below that of the corresponding solvated energies of TS1–TS3. Only one significant discrepancy with experimental observation remains; namely that solvation also reduces the energy of TS4 (M = Zn) to below that of TS3 (L = OTf).¹² Nevertheless, these calculations do provide an insight into how the variation in metal coordination can result in differing selectivity by the metals.

To conclude, regioselective cyclisation of γ -allenols can be directed by Lewis acids *via* divergent pathways: while Ag catalysis proceeded *via* a 5-*exo*-trig pathway, 6-*exo*-dig cyclisation is favoured by Sn and Zn catalysts. Calculations of relative energies of transition states revealed that kinetic control is attained by varying metal geometry and ligand/counterion.

We thank EPSRC and Zambon Advanced Fine Chemicals (ZaCh Systems S.A.) for studentship support.

Notes and references

- R. W. Bates and V. Satcharoen, *Chem. Soc. Rev.*, 2002, **31**, 12.
- (a) H. Qian, X. Q. Han and R. A. Widenhoefer, *J. Am. Chem. Soc.*, 2004, **126**, 9536; (b) Z. B. Zhang, C. Liu, R. E. Kinder, X. Q. Han, H. Qian and R. A. Widenhoefer, *J. Am. Chem. Soc.*, 2006, **128**, 9066.
- (a) G. L. Hamilton, E. J. Kang, M. Mba and F. D. Toste, *Science*, 2007, **317**, 496; (b) Z. B. Zhang and R. A. Widenhoefer, *Angew. Chem., Int. Ed.*, 2007, **46**, 283.
- endo*-Cyclisation of activated allenols was achieved using 1.5 equivalents of *t*-BuOK: C. Mukai, M. Ohta, H. Yamashita and S. Kitagaki, *J. Org. Chem.*, 2004, **69**, 6867.
- X. H. Yu, S. Seo and T. J. Marks, *J. Am. Chem. Soc.*, 2007, **129**, 7244.
- For our prior work, see: (a) L. A. Adrio and K. K. Hii, *Chem. Commun.*, 2008, 2325; (b) P. H. Phua, S. P. Mathew, A. J. P. White, J. G. de Vries, D. G. Blackmond and K. K. Hii, *Chem.–Eur. J.*, 2007, **13**, 4602; (c) J. G. Taylor, N. Whittall and K. K. Hii, *Org. Lett.*, 2006, **8**, 3561; (d) J. G. Taylor, N. Whittall and K. K. Hii, *Chem. Commun.*, 2005, 5103.
- Regiodivergent (5-*endo*vs. 7-*endo*-trig) cyclisation of γ -allenols had been reported, but different protecting groups were deployed on the precursors: B. Alcaide, P. Almendros and T. M. del Campo, *Angew. Chem., Int. Ed.*, 2007, **46**, 6684.
- Reactions were reported by using 1.2–2 eq. of AgNO₃: P. Audin, A. Doutheau, L. Ruest and J. Goré, *Bull. Soc. Chim. Fr.*, 1981, 313.
- After the submission of this manuscript, triflic acid-catalysed reactions of **1a** to **4** was reported to proceed in refluxing CH₂Cl₂ (20 mol%, 5 h, 80% yield). The crystal structure of **4** was also reported: K. Mori, S. Sueoka and T. Akiyama, *Chem. Lett.*, 2009, **38**, 628. We are grateful to Prof. Akiyama for bringing the reference to our attention.
- Retention of ring aromaticity despite having 4-coordination at one of the ring carbons is a known phenomenon, see: (a) R. J. Wehmschulte, B. Twamley and M. A. Khan, *Inorg. Chem.*, 2001, **40**, 6004; (b) E. Solari, F. Musso, E. Gallo, C. Floriani, N. Re, A. Chiesi-Villa and C. Rizzoli, *Organometallics*, 1995, **14**, 2265; (c) N. Choi, P. D. Lickiss, M. McPartlin, P. C. Masangane and G. L. Veneziani, *Chem. Commun.*, 2005, 6023.
- S. I. Gorelsky, D. Lapointe and K. Fagnou, *J. Am. Chem. Soc.*, 2008, **130**, 10848, and references cited therein.
- Advances in computational solvation methodologies will allow solvation potential surfaces to be more effectively explored and the origins of such discrepancies probed: D. M. York and M. Karplus, *J. Phys. Chem. A*, 1999, **103**, 11060, as implemented in Gaussian09.